European Journal of Radiology Open 4 (2017) 27–39

Contents lists available at ScienceDirect

European Journal of Radiology Open

journal homepage: www.elsevier.com/locate/ejro

The accuracy and sensitivity of diffusion-weighted magnetic resonance imaging with Apparent Diffusion Coefficients in diagnosis of recurrent cholesteatoma

Nasr Mohamed M. Osman[a,*], Ahmed Abdel Rahman[b], Moustafa Talaat Abdel Hakim Ali[b]

[a] Department of Radiology, Minia University Hospital, Minia, Egypt
[b] Department of Otolaryngology, Minia University Hospital, Minia, Egypt

ARTICLE INFO

Article history:
Received 16 January 2017
Received in revised form 24 February 2017
Accepted 10 March 2017
Available online 23 March 2017

Keywords:
Recurrent cholesteatoma
Magnetic Resonance Diffusion weighted imaging
Apparent diffusion coefficient
Multidetector computed tomography

ABSTRACT

Objective: To evaluate the accuracy and sensitivity of diffusion-weighted magnetic resonance imaging with ADC value combined with MDCT in evaluating recurrent cholesteatoma.
Patients: Thirty patients (20 females and 10 males), their age ranged from 10 to 40years, had undergone a tympanomastoid surgery for a cholesteatoma of the middle ear underwent MDCT and MR DWI examination before second- or third-look surgery from May 2015 to October 2016.
Results: CT showed partial opacification of the tympanomastoid cavity in 10 ears and complete opacification in 21 ears. CT detects 10 cases out of 20 cases of recurrent cholesteatoma with sensitivity 47.6%, specificity 100%, and NPP 47.6%. DWI depicted 21 out of 20 cases proved cholesteatoma patients (sensitivity 100%, specificity 90%, PPV 95.2% and P value is 0.001). All MRI of patients without cholesteatoma were correctly interpreted as showing negative findings for cholesteatoma (specificity = 100%). The ADC of cholesteatoma group (21 ears) were ranged from 553 to 759×10^{-3} mm^2/s and the ADCs of non cholesteatoma group (10 ears) was ranged from 1495.8 to 1766.8×10^{-3} mm^2/s. Cut off value of cholesteatoma is $\leq 759 \times 10^{-3}$ mm^2/s.
Conclusion: MR DWI with ADC combined with MDCT has high sensitivity, specificity, accuracy in detecting recurrent cholesteatoma.

1. Introduction

Middle ear cholesteatoma is a benign cystic lesion of aggressive behavior which requiring prompt surgical treatment to prevent local and intracranial complications [1]. Surgery is the mainstay treatment of cholesteatoma However, the risk of residual cholesteatoma and recurrence occurs in a relatively high numbers of patients, whatever the type of surgery used [2,3]. The detection of cholesteatoma in patients who have undergone middle ear surgery is often difficult for the follow-up of patients operated for cholesteatoma [4]. High resolution computerized tomography (CT) scan is considered the basic method for imaging the nonoperated middle ear and can be complemented by magnetic resonance imaging (MRI) [3–6]. However, following mastoid surgery, both imaging modalities cannot reliably distinguish residual or recurrent disease from postoperative changes such as granulation tissue, fluid or fibrous tissue [6].

Diffusion-weighted (DW) sequences are highly promising in differentiating recurrent cholesteatoma from granulation tissue DW MRI depends on the difference in diffusion of water molecules in different biological tissues. Water molecules in cholesteatoma are less mobile giving rise to a hyperintense signal. In granulation tissue, water molecules are more mobile and thus appear less intense on DW sequence [7,8].

Currently, single-shot echo-planar DWI is the most used DWI technique because of its short imaging time (about 2 min). On the other hand, multi-shot non-echo-planar DWI sequences requiring a longer imaging time are associated with decreased susceptibility artifacts [7,8].

The ADC map is free from T1 or T2 effects, and provides a true quantitative display of water diffusion at each voxel [9,10]. ADCs, have not yet been assessed as a diagnostic criterion for the detection of recurrent middle ear cholesteatoma with no clear-cut values exist for differentiation of recurrent cholesteatoma from granulation tissue or fibrosis [11–15]. In this study, we aim to determine

* Corresponding author.
E-mail address: nasrosman_7@yahoo.com (N.M.M. Osman).

http://dx.doi.org/10.1016/j.ejro.2017.03.001

Table 1
Clinical presentations of 30 patients (31 ears).

Clinical presentation	No. of patients	%
Chronic purulent ear discharge	25	83.4
Chronic discharge with tympanic membrane perforation	3	10
Chronic discharge with signs of increased I.C.T	1	3.3
Chronic discharge with facial paresis	1	3.3
Total	30	100

Table 2
CT findings of 30 patients with previous tympanomastoid surgery (31 ears).

CT finding	No. of patient	%
Type of surgery performed		
Canal wall up	17	54.8 45.2
Canal wall down	14	
Tissue density mass		
Partial opacification	10	32.3
Complete opacification	21	67.7
Size of the tissue density mass	10 mm 30 mm	
Ossicular chain		
Intact	6	19.4
No ossicles	25	80.6
Associated Bony erosion		
Eroded tegmen	1	3.2
Eroded sigmoid sinus plate	1	3.2
Eroded facial nerve canal	1	3.2
Eroded lateral mastoid wall	3	9.6
The other (sound) ear		
Normal	25	83.4
CSOM	4	13.3
Cholesteatoma	1	3.3

the diagnostic accuracy of DWI and the difference between the ADCs of postoperative middle ear cleft cholesteatoma and those of non-cholesteatomatous tissue on single-shot echo planar DW images.

2. Patients and methods

The study was approved by the institutional review board and informed consent was obtained from all patients. We included 30 consecutive patients in our study, previously subjected to tympanomastoid surgery for the treatment of cholesteatoma with clinical and CT suspicion of recurrence and scheduled for second look operation, during the period from May 2015 to October 2016. Twenty patients were females and 10 were males, with an age ranging from 9 to 45 years old (mean = 27 years). One patient had bilateral middle ear surgery for cholesteatoma. Canal wall-up technique was already done for 17 ears, while 14 ears had canal wall-down technique. The main clinical presentation of the patients was a recurrent purulent discharge (n = 25), perforated tympanic membrane with and without discharge (n = 3), chronic ear discharge with sign of increase intracranial tension (n = 1), chronic discharge with facial paresis (n = 1) (Table 1). All patients were scheduled for revision surgery and the intraoperative findings were compared to imaging results.

The mean interval between the first tympanomastoid surgery and CT examination was 12–30 months; all patients were further assessed by MRI imaging of the petrous temporal bone on an average of 1–2 weeks after CT examination. Positive cases of recurrent cholesteatoma were referred for second-look surgery, while −ve cases received medical treatment. The second-look surgery was performed within 2–3weeks after the MR examination.

Inclusion criteria include: Patient with history of tympanomastoid surgery for cholesteatoma with clinical suspicion of recurrent cholesteatoma or infection during follow-up.

Exclusion criteria include: patient with unclear operative history, active infection or mastoid abscess.

2.1. All patients are subjected

1. **Full history taking including**: Age, sex, chronic ear discharge, conductive hearing loss, headache, vomiting (signs of increased intracranial tension) and facial palsy.
2. **Through clinical examination**: All Patients are subjected to otoscopic examination at the ENT Department.
3. **Operative history**: (mastoidectomy, otoscope and otoendoscope)

4.1: MDCT examination using multi-detector CT scanner 16 channel (GE CT/Bright speed Elite scanner, General Electric Medical System, USA).

CT technique: The images were obtained with 0.5 mm collimation, 0.5 mm thickness, 320 mAs, and 120kVp. The obtained data was reconstructed in the axial plane using high resolution bone algorithm (extended window sitting at around 4000HU and window level around 300HU) with 0.5 mm section thickness, 0.05 mm increments, and a FOV of 100, with a matrix size of 512 × 512. At this collimation, an isotropic voxel (which measure 0.5 mm per side) was obtained. The axial data were then transferred to a separate workstation for post-processing, with a commercially available 3D reformatting software (Baxara 3D). Sections was taken at 1 mm increments beginning at the level of the floor of hypotympanum and jugular fossa extending to the level of arcuate eminence using line for localization.

4.2: MRI examinations were performed with 1.5-T MRI unit (Philips, Achiva, Philips Medical Systems, Eindhoven, Netherlands) following patients' informed consent and exclusion of contraindications. The following sequences were acquired on the middle ear using an 8 channel head coil and applying the Parallel SENSE imaging is used to obtain better resolution, faster dynamic scans and to reduce susceptibility artifacts. DWI parameters includes (FOV, 230 × 230 mm; Epi factor, 61; thickness/gap, 5/1 mm; acquisition matrix, 112 × 89) was performed by using b values of 800 and 1000 s/mm^2 in axial, multisection, single-shot, echo-planar imaging sequence. TE was taken as short as possible for the acquisition of the highest signal-to-noise ratio. The ADC maps were reconstructed with commercially available software.

The following sequences were acquired on the middle ear.

1. 3D CISS (constructive interference in steady state) with a gradient echo component tilt angle: 70°, slice thickness: 0.7 mm,

Table 3
Sensitivity and specificity of MR DWI, MDCT, both, operative in diagnosing recurrent cholesteatoma.

Examination	Recurrent cholesteatoma	Sensitivity	Specificity	PPV	NPP
MR DWI	21	100%	90.9%	95.2%	100%
MDCT	10	50%	100%	100%	52.4%
Combined DWI and MDCT	21	100%	90.9%	95.2%	100%
Operative	20	100%	100%	100%	100%

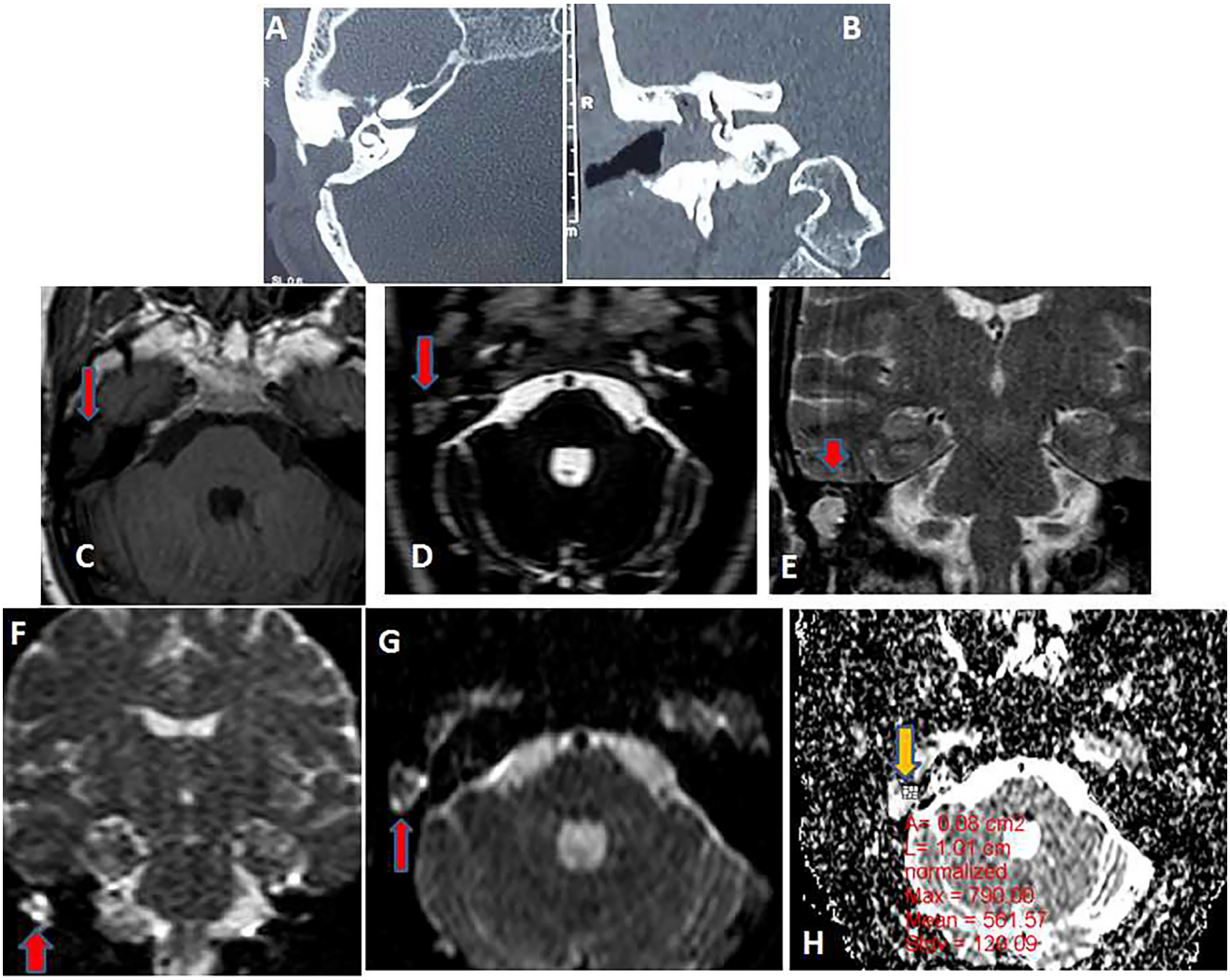

Fig. 1. Recurrent cholesteatoma in the right middle ear of 45y old woman who underwent CWU middle ear surgery. (A and B) Axial and coronal CT cuts showed complete opacification of the right middle ear cleft by tissue density lesion associated with eroded ossicular chain and bulging tympanic membrane outwards. (C) Axial T1WI, (D) Axial CISS and (E) Coronal T2W conventional non contrast MRI showed a soft tissue lesion in the right middle ear cleft of hypointense signal at T1WI and high signal intensity in T2WI and CISS. (F, G) Coronal and axial diffusion-weighted fast SE image obtained with a b factor of 1000 s/mm^2 showed high signal intensity of the cholesteatoma. (H) ADC (mean 561.75 $\times$ 10^{-3} mm^2/s). The lesion size is 1.5 cm at CT and 1 cm at DWI.

repetition time (TR): 11.5 ms, echo time (TE): 5.75 ms, SENSE factor 2, FOV: 230 mm. Acquisition time 3 min and 50 s.

2. Axial and coronal echo planar single shot turbo spin echo diffusion-weighted imaging: 2.5 mm thick axial slices, TE: 98 ms, TR: 2000 ms, SENSE factor 2, diffusion factor: B 1000 s/mm^2, FOV: 230 mm. Acquisition time 2 min and 50 s,
3. Axial T1 and T2-weighted coronal spin echo (TSE). TR/TE, 5270/119 ms; matrix, 512; section thickness, SENSE factor 2, 3 mm; field of view, 230 mm. Acquisition time 3 min and 12 s.

The ADC value of the cholesteatoma was calculated on the ADC map from the selected region of interest (ROI) that matched the lesion. The image section for ROI placement was selected and the ROI drawn by the reading radiologist. The image for ROI placement was selected to avoid the edges of the lesion and partial volume averaging, so the central aspect of the lesion was targeted. If the lesion is of small size, the mean ADC of the lesion was taken from ROIs on the two contiguous sections. Repeated ROI measurements were done two to three times on the image for each case, and the median ADC was obtained.

2.2. Imaging evaluation

All imaging, whether CT or MRI, was prospectively interpreted by the same radiologist, specifically trained in petrous bone imaging for about 15 years experience. On CT, recurrent cholesteatoma was diagnosed by identifying the presence of new bone erosion not detected in the preoperative evaluation, the presence of tissue density mass with well-defined borders and an air space between the mass and walls of the tympanic cavity, expansion of the mastoidectomy cavity and erosion of the walls including the tegmen, ossicular chain amputation, or labyrinthine or facial nerve sheath destruction that could not be attributed to past surgery. Images were considered negative for cholesteatoma when middle ear cavities were either air filled or showed minimal thickening. Interpretation was indeterminate, whenever complete opacification of the tympanomastoid cavity.

On MRI sequences, the diagnosis of cholesteatoma was based on identifying area of restricted diffusion in the form of marked hyperintense signal in comparison with brain tissue on the b = (800, 1000) images of diffusion-weighted. The radiologist classified MRI results into two groups (recurrent cholesteatoma or non-cholesteatomas). Lesion dimension at maximum diameter on axial and coronal

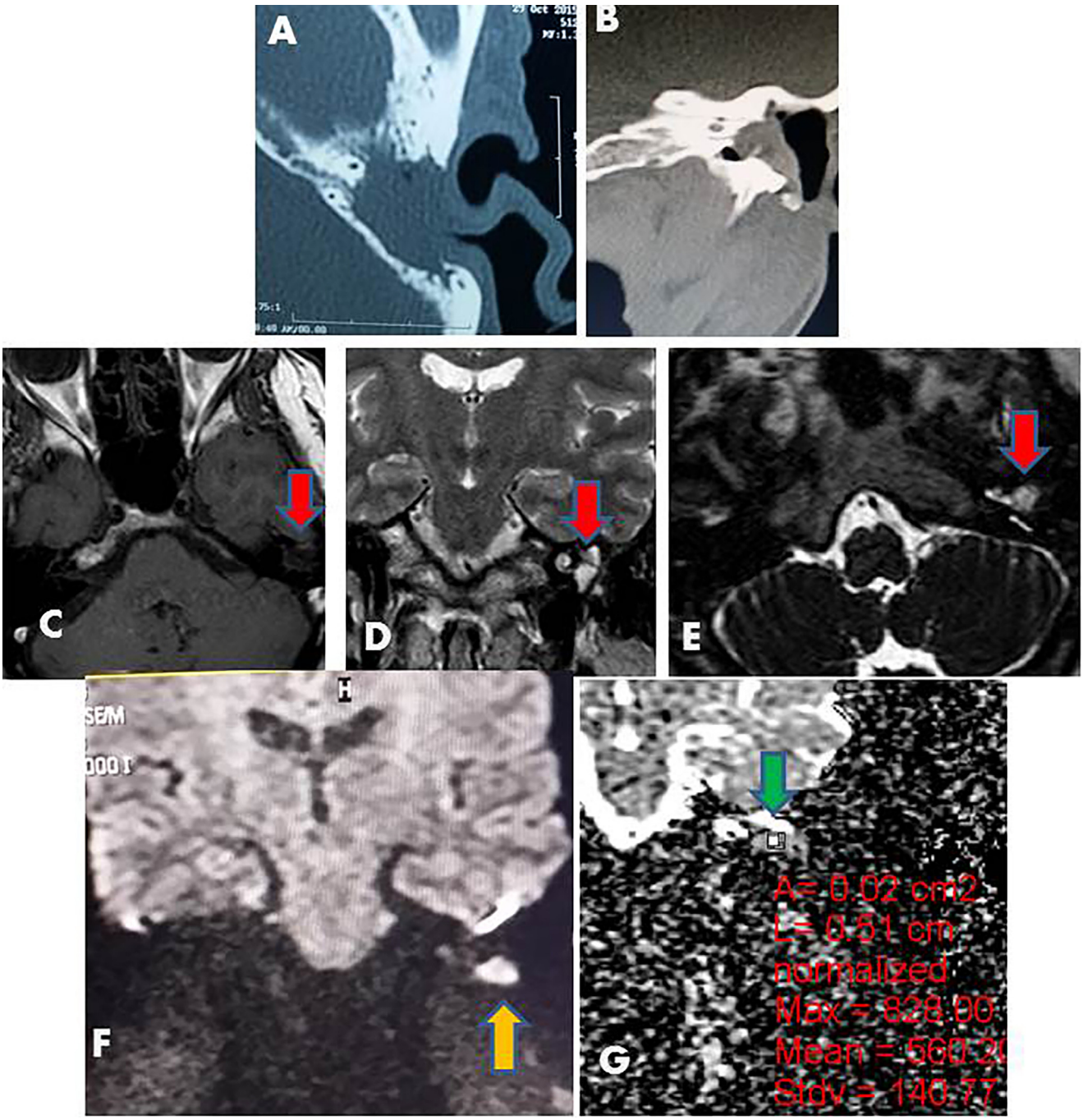

Fig. 2. Recurrent cholesteatoma in the left middle ear of a 50y old woman who underwent CWD ear surgery. (A and B) Axial and coronal CT cuts revealed complete opacification of the right middle ear cleft, absent ossicules. (C) Axial T1WI, (D) Axial CISS and (E) Coronal T2W MRI sequences showed a soft tissue lesion in the right middle ear cleft of hypointense signal at T1WI and high signal intensity at T2WI and CISS (Red arrow). (F) Coronal DWI fast SE image obtained with a b factor of 1000 s/mm^2 showed markedly high signal intensity of the cholesteatoma (yellow arrow). (G) ADC (mean 566 $\times$ 10^{-3} mm^2/s), (green arrow). The lesion size is 2 cm at CT and 1 cm at DWI.

planes was also recorded on MRI and CT and compared with that of operative finding.

The surgical findings were obtained from the surgical reports of one team of otology surgeons. The surgical results were classified as recurrence of cholesteatoma or no recurrence of cholesteatoma (granulation tissue). All patients were scheduled for revision surgery and the intraoperative findings were compared to imaging results. The sensitivity, specificity, positive and negative predictive values of different MR sequences used and ADCS, was assessed using SSPS (version 12).

3. Results

This prospective study was conducted in 30 patients with 31ears as one patient had bilateral tympanomastoid surgery for cholesteatoma.

3.1. Demographic and clinical data

We evaluated 30 consecutive patients (31 ears), 20 were females and 10 males, their age ranged from 9–45 years, mean age 27 years, who had undergone a canal wall-down mastoidectomy or a canal

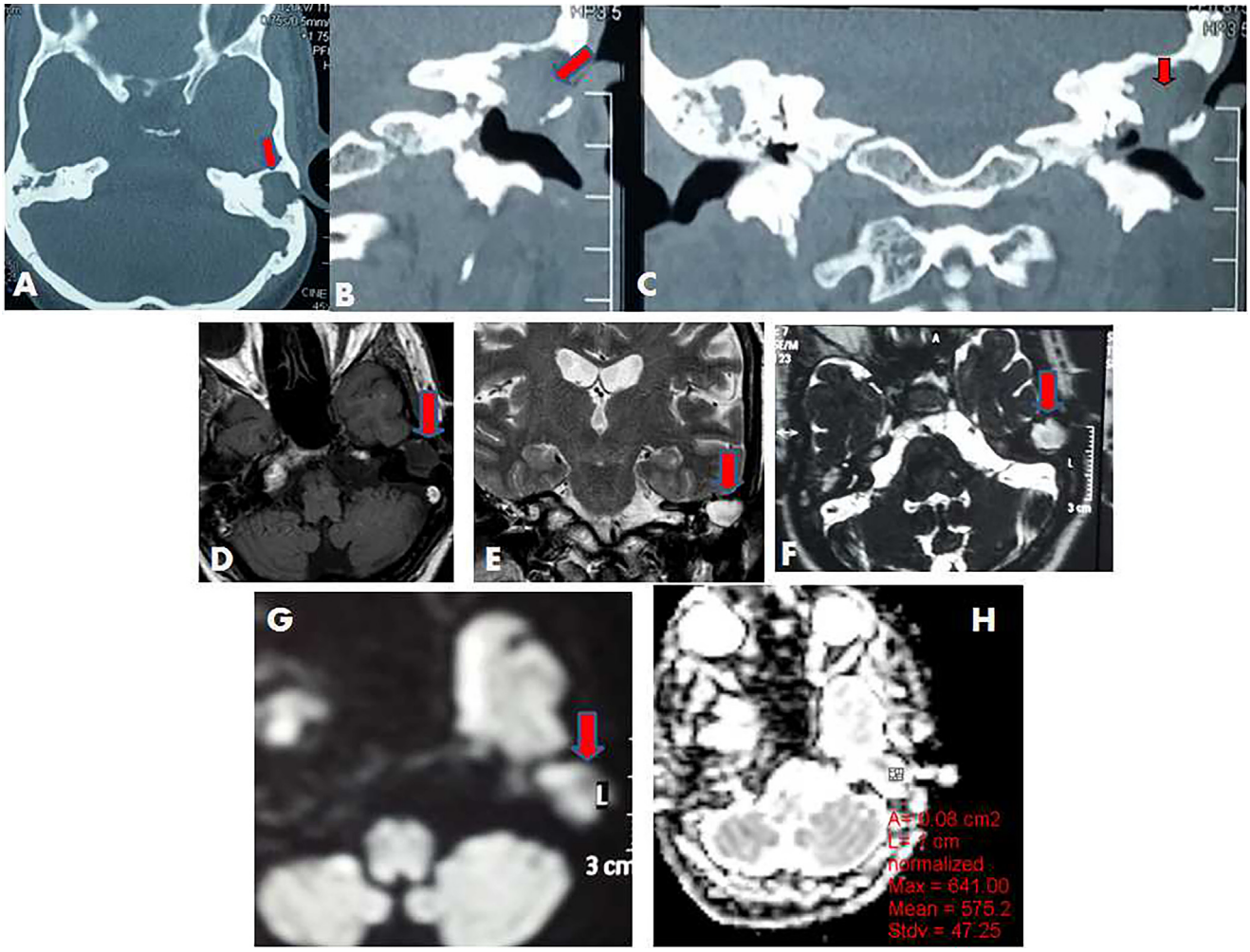

Fig. 3. Recurrent cholesteatoma in the left middle ear of a 38 years old man who underwent canal wall up middle ear surgery. (A–C) Axial and Coronal CT cuts showed complete opacification of the left middle ear cleft (red arrow) with absent ossicles. (D) Axial T1WI, (E) Coronal T2W and axial (F) CISS MRI sequences showed a soft tissue lesion in the left middle ear cleft of low signal at T1WI and high signal intensity at T2WI and CISS (red arrow). (G) Axial DWI obtained with a b factor of 1000 s/mm^2 showed high signal intensity of the cholesteatoma (red arrow). (I) ADC (mean 575 × 10^{-3} mm^2/s). The lesion size 16 mm, 9 mm.

wall-up mastoidectomy for a cholesteatoma of the middle ear and underwent an MDCT and MR DWI examination before second-look operation.

The main clinical presentation of the patients were recurrent purulent discharge (n = 25), perforated tympanic membrane with and without discharge (n = 3), chronic ear discharge with sign of increase intra cranial tension (n = 1), chronic discharge with facial paresis (n = 1). Canal wall-up technique was done for 17 ears, while 14 ears had canal wall-down technique. One patient had bilateral operation (Table 2).

3.2. MDCT findings (Table 2)

CT scan showed partial opacification of the tympanomastoid cavity in 10 ears (Figs. 3 and 5) and complete opacification in 21 ears (Figs. 1, 2, 4, 6 and 8). The left ear was affected in 26 patients (Figs. 2–6 and 8) and the right was affected in 5patients (Figs. 1 and 5). CT criteria of recurrent cholesteatoma detected in 10 cases in the form of localized nondependent tissue density mass with new bone erosion not detected in previous CT or pre-operative study (Fig. 10), while the remaining 20 cases the mastoiedctomy cavity was completely opacified. The size of cholesteatoma mass lesion ranged from 10 to 30 mm (mean17.8 ± 5.7 mm). Ossicular chains were intact in 6 ears and not visualized (eroded or amputated) in 25 ears. The tegmen tympani was eroded in one case, sigmoid sinus plate eroded in one case, tympanic segment of the facial nerve canal was eroded in one case, and lateral mastoid wall was eroded in one case (Fig. 10). The other ear was normally aerated in 25 ears and revealed chronic suppurative otitis media in 4 ears (Figs. 3, 4 and 6), bilateral cholesteatoma detected in one case (Fig. 5). Based on CT criteria of recurrent cholesteatoma, 10 cases were accurately diagnosed.

3.3. MRI and MR DWI findings (Tables 3 and 4)

Based on MRI findings the included patients were classified into two groups, (cholesteatoma group include 20 cases) and non cholesteatoma group (include 10 cases). All patients showed low signal intensity on unenhanced T1WI, high signal intensity on T2WI and 3DCISS sequences. Based on MR DWI sequence, the cholesteatoma group (20 patients with 21 ears) revealed recurrent cholesteatoma in the form of area of restricted diffusion on DW images at b factor of 800, 1000 s/mm^2 (Figs. 1–4, 6 and 8). Patients without recurrent cholesteatoma (10 patients), all diffusion-weighted fast SE MR images obtained with b of 800,1000 s/mm^2 were correctly interpreted as showing no restriction and were diagnosed as granulation or infection (Fig. 7). The size of the recurrent cholesteatoma mass was ranged from

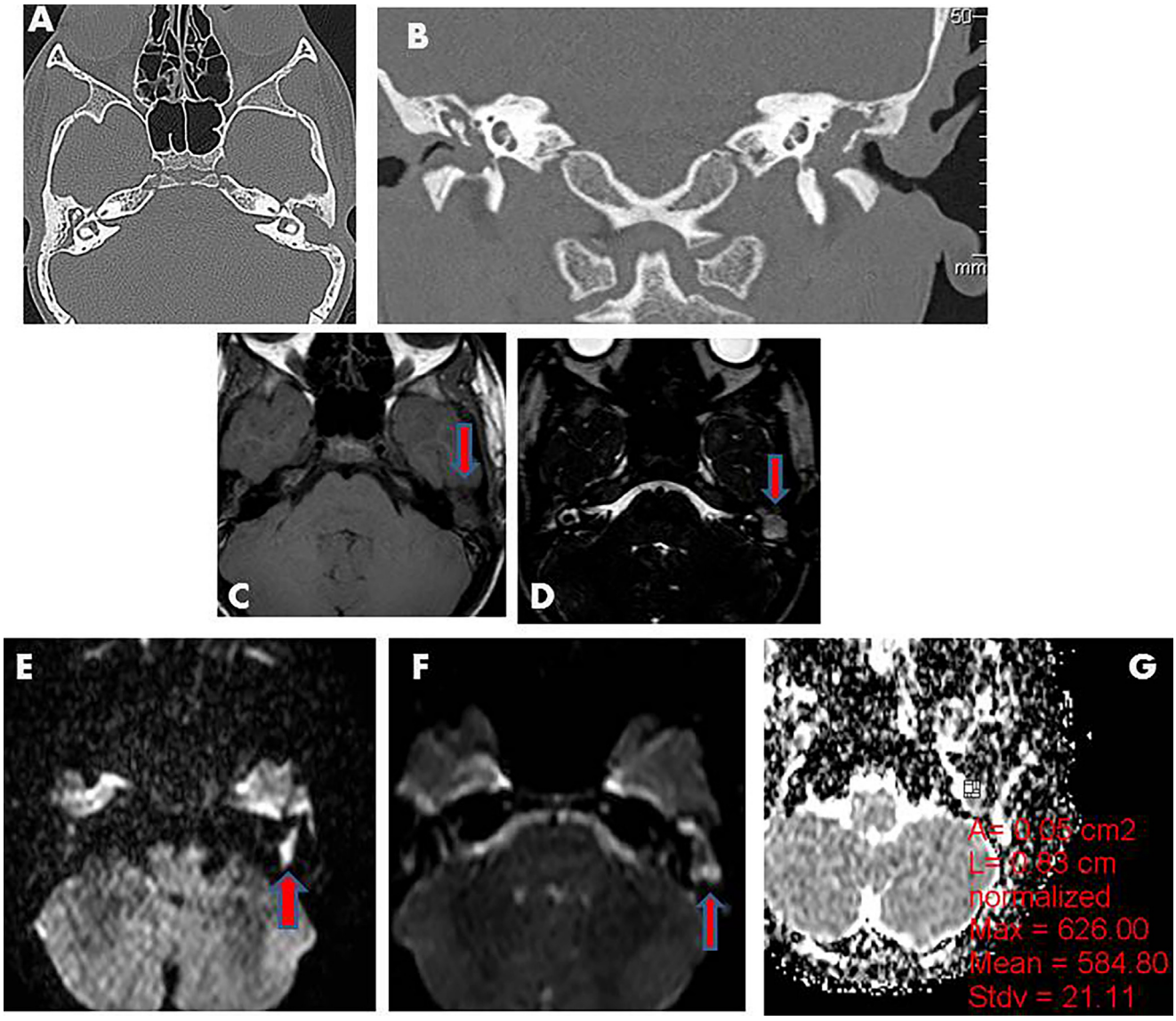

Fig. 4. Recurrent cholesteatoma in the left middle ear of a 12y boy who underwent ICW middle ear surgery. (A and B) Axial and coronal CT cuts showed complete opacification of the left middle ear cleft by tissue density lesion associated with erosion of the ossicular chain. (C, D) Axial T1WI, axial CISS showed a soft tissue lesion in the left middle ear cleft of low signal in T1WI and high signal intensity in T2WI (red arrow). (E, F) Axial DWI obtained with a b factor of 1000 s/mm^2 showed markedly high signal intensity of the cholesteatoma (red arrow). (G) ADC (mean 584×10^{-3} mm^2/s). The size of the lesion is 15 mm at CT and 10 mm at MRD. The right ear showed CSOM.

Table 4
Comparison between CT, MR DWI and operative in diagnosis of recurrent cholesteatoma (21ears).

Examination	MR DWI	MDCT	Operative	P1	P2
Recurrent cholesteatoma	21(100%)	10(47.6%)	20(100%)	0.5	0.001*
Total	21(100%)	21(100%)	20(100%)		

P1 = MR DWI versus operative, p2 = MDCT versus operative.

10–30mmat CT, 7–15 mm at MR DWI and 7–14 mm at operative finding (Table 9). There was one false-positive case measures 9 × 6-mm related to LSC that was not a recurrent cholesteatoma but bone graft placed during the initial surgery to seal a lateral semicircular canal fistula (Fig. 9). The positive predictive value was 95.2% (21 of 20 patients).

3.4. CECs values: Tables 5–7

The ADC values of cholesteatoma group (21 ears) were ranged from 553 to 759×10^{-3} mm^2/s), Mean $\pm$SD611.8 $\pm$ 51.8 $\times 10^{-3}$ mm^2/s) and median 595×10^{-3} mm^2/s). The ADCs of non cholesteatoma group (10 ears) was ranged from 1495.8 to 1766.8 $\times 10^{-3}$ mm^2/s, Mean 1638.3 $\pm$ 93.5 $\times 10^{-3}$ mm^2/s and median 1653.5×10^{-3} mm^2/s. The cut off value of cholesteatoma is $\leq 759 \times 10^{-3}$ mm^2/s (Table 8).

3.5. MR DWI, MDCT versus operative diagnosis of recurrent cholesteatoma

Surgery proves the diagnosis of recurrent cholesteatoma in 20 patients (20 ears). Large recurrence seen in attico-antral region were found in 10 ears, the largest lesion reached 30 mm at CT, 14 mm at MR DWI and 14.4 mm operative size (Figs. 2 and 3),

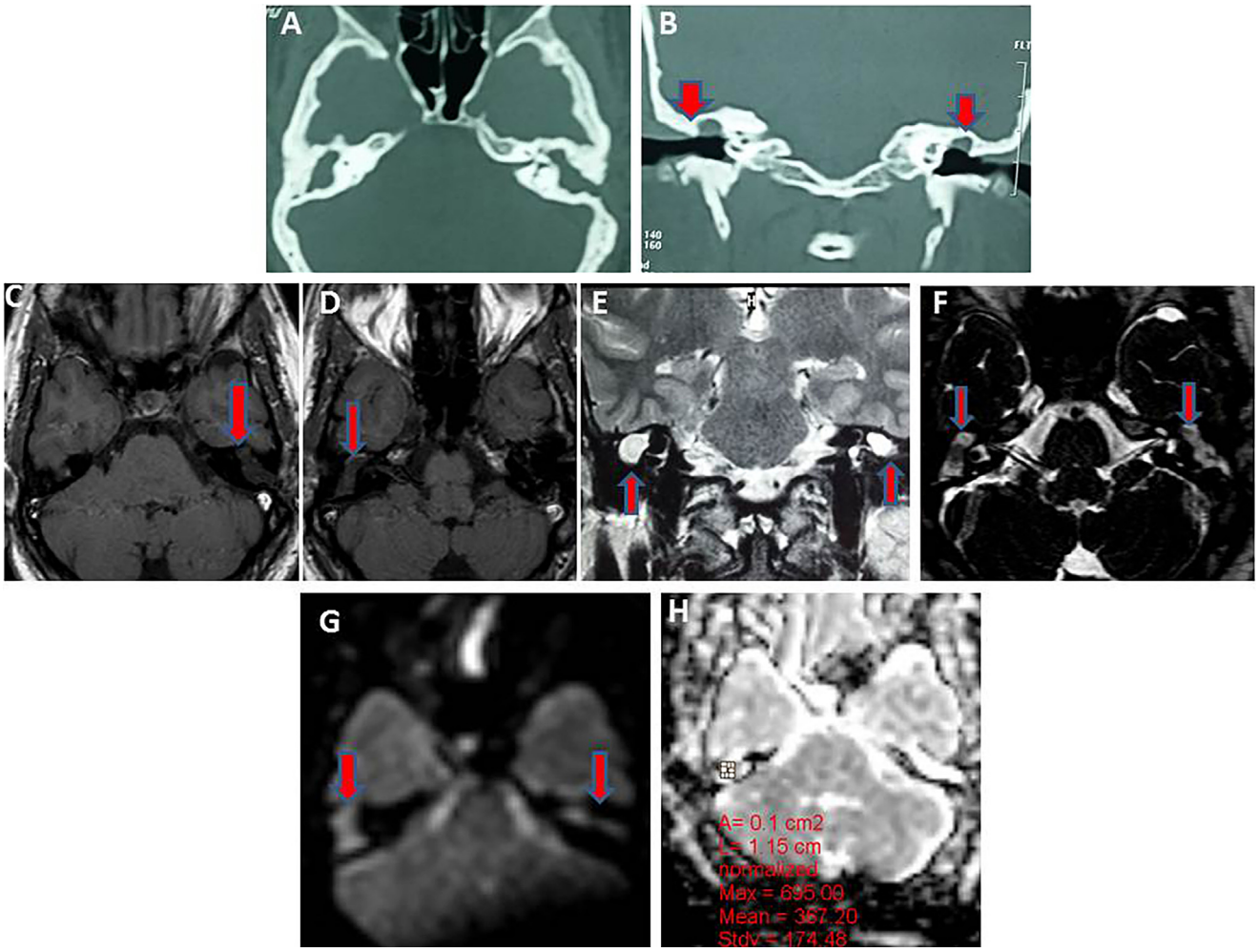

Fig. 5. Bilateral recurrent cholesteatoma of a 33y old woman who underwent CWU middle ear surgery at both sides. (A and B) Axial and coronal CT cuts showed opacified attic on both sides by non-dependent tissue density lesion associated with absent ossicles (red arrow). (C) Axial T1WI right and (D) left ear, (E) Axial CISS and (F) Coronal T2W SE showed a soft tissue lesion in the middle ear cleft of both ears of low signal in T1WI and high signal intensity in T2WI and CISS (red arrow). (G) Axial DWI fast SE image obtained with a b factor of 1000 s/mm^2 showed markedly high signal intensity of the cholesteatoma on both sides (red arrow).(H) ADC (mean 759, 724 × 10^{-3} mm^2/s).

Table 5
ADC values of recurrent Cholesteatoma patients (n = 21) and non cholesteatomatous patient (n = 10).

Case	Recurrent Cholesteatoma ADC Value ($\times 10^{-3}$ mm^2/s)	non cholesteatomatous ADC Value ($\times 10^{-3}$ mm^2/s)
1	560	1651.62
2	575	1655.45
3	595	1766.85
4	563	1717.64
5	633	1748.67
6	578	1495.88
7	584	1594.55
8	643	1519.39
9	626	1554.66
10	595	1678.55
11	553	
12	759	
13	634	
14	641	
15	724	
16	574	
17	602	
18	641	
19	603	
20	582	
21	583	

Table 6
ADC values of recurrent cholesteatoma patients (n = 21) and non-cholesteatoma patients (n = 10).

ADC	recurrent cholesteatoma ADC Value ($\times 10^{-3}$ mm^2/s)	non cholesteatoma ADC Value ($\times 10^{-3}$ mm^2/s)	P
Range	553–759	1495.8–1766.8	0.001*
Mean ± SD	611.8 ± 51.8	1638.3 ± 93.5	
Median	595	1653.5	

medium sized recurrence in 8 cases, while smaller recurrences were seen in the middle ear cavity in 3 ears, reaching 10 mm at CT, 7 mm at MR DWI and 7.3 mm at the operation (Fig. 9), Table 9. The lesion sizes at CT was not correlated with that of the MR DWI and operative because CT gives apparent size of cholesteatoma including the surrounding granulation tissue while the size at MR DWI and operative was more accurate excluding the surrounding granulation tissue with significant (P value = 0.001*). Granulation tissue, fibrosis and secretions were found in the remaining 10 ears (Fig. 7), Tables 3 and 4.

Good correlation between MR DWI finding and operative confirmation, the sensitivity was 100%, the specificity was 90%, the

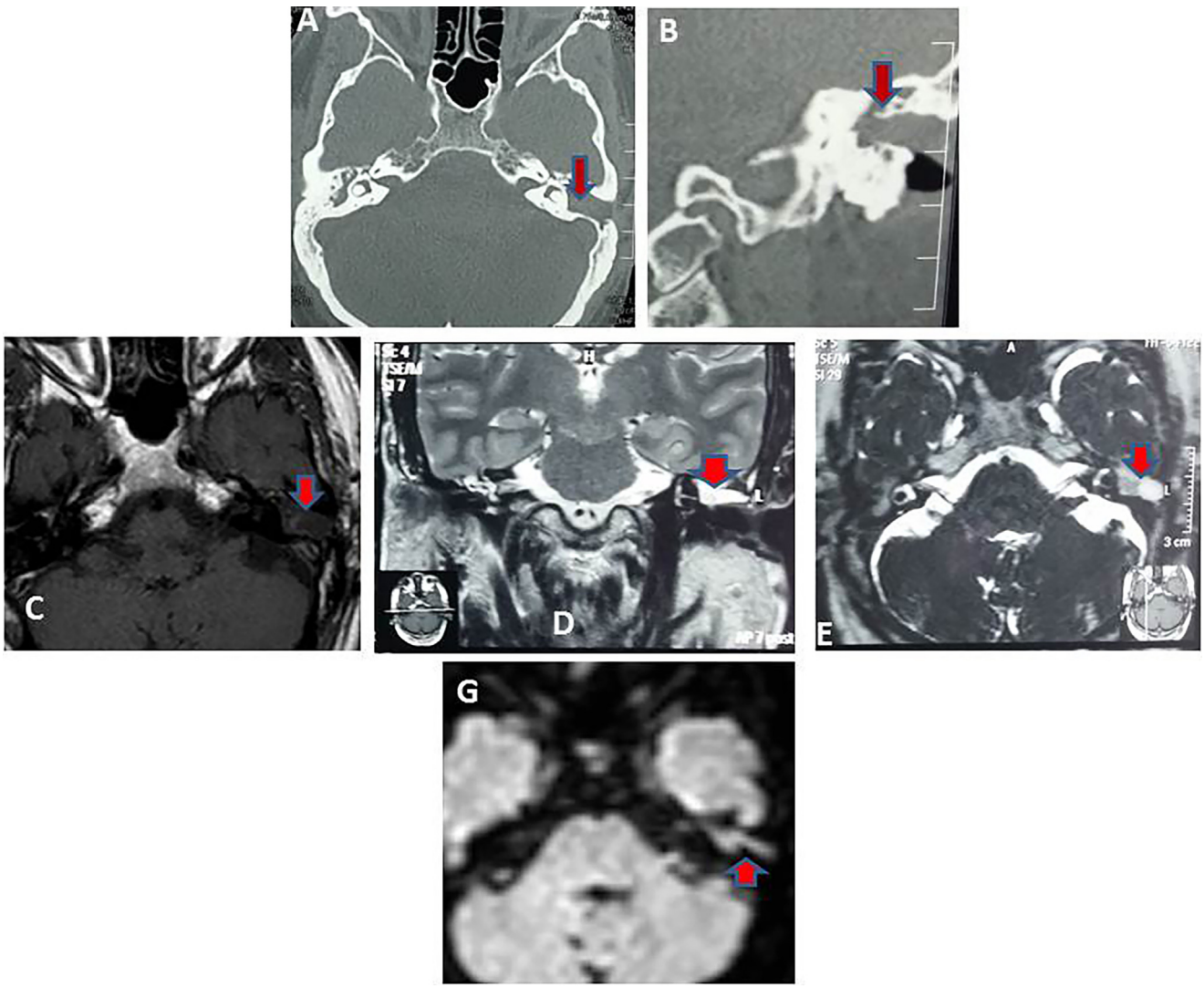

Fig. 6. Recurrent cholesteatoma in the left middle ear with CSOM at the right of a 38 years old man who underwent CWU middle ear surgery. (A and B) Axial and coronal CT cuts showed complete opacification of the right middle ear cleft by tissue density lesion associated with eroded ossicular chains (red arrow). (C) Axial T1WI, (D) Coronal T2W SE and (E) Axial CISS showed a soft tissue lesion in the right middle ear cleft of low signal at T1WI and high signal intensity at T2WI and CISS. (G) Axial DWI obtained with a b factor of 1000 s/mm^2 showed high signal intensity of the cholesteatoma (red arrow) at the left with no abnormal signal at T2WI. The size of the lesion is 18 mm at CT and 11 mm at DWI.

positive predictive value 95.2% and P value is 0.001. MDCT had low sensitivity, detect only 10 cases out of 30 cases, the sensitivity was 47.6%, specificity 100%, and negative predictive value 47.6% and P value is 0.5 (Table 5).

4. Discussion

Diagnosis of recurrent cholesteatoma in an operated middle ear cavity may be difficult. High resolution CT scan and conventional MRI have low specificity when it comes to differentiating granulation tissue from relapsing cholesteatoma due to lack of characterization of the detected soft tissue in the surgical cavity [9–13] (Fig. 11).

Our study depict low specificity and accuracy of MDCT (47.6%), this results is near the result of Adam et al. [16] who studied 41 patients underwent revision tympanomastoidectomy with sensitivity 50% and specificity 43% for the recurrent well defined mass. CT could not confirm the diagnosis of recurrent cholesteatoma in completely opacified tympanomastoid cavity and could not differentiate between recurrence, residual and granulation tissue. CT has widely been accepted for assessing the extent and location of disease and evaluating complications of cholesteatomas. Preoperative imaging is especially important for demonstrating disease in hidden areas (such as the sinus tympani and facial recess) and extension of disease into the epitympanum (attic) and mastoid antrum, and for detecting normal anatomic variations (such as an aberrant course of the facial nerve). CT is useful if no soft tissue is seen in the middle ear (or petrous apex or mastoid depending on original location of disease). If rounded soft tissue is present, then findings are suggestive of recurrent disease. However, if amorphous soft tissue or complete middle ear opacification is present, CT is nonspecific and cannot distinguish granulation tissue or scar tissue from recurrent disease [17].

The importance of diffusion-weighted MR imaging in the detection of recurrent cholesteatoma has been reported in several previous studies [14,18]. Cholesteatoma has high signal intensity on diffusion-weighted images obtained with b factors of 800 or 1000 s/mm^2, whereas granulation tissue has low signal intensity

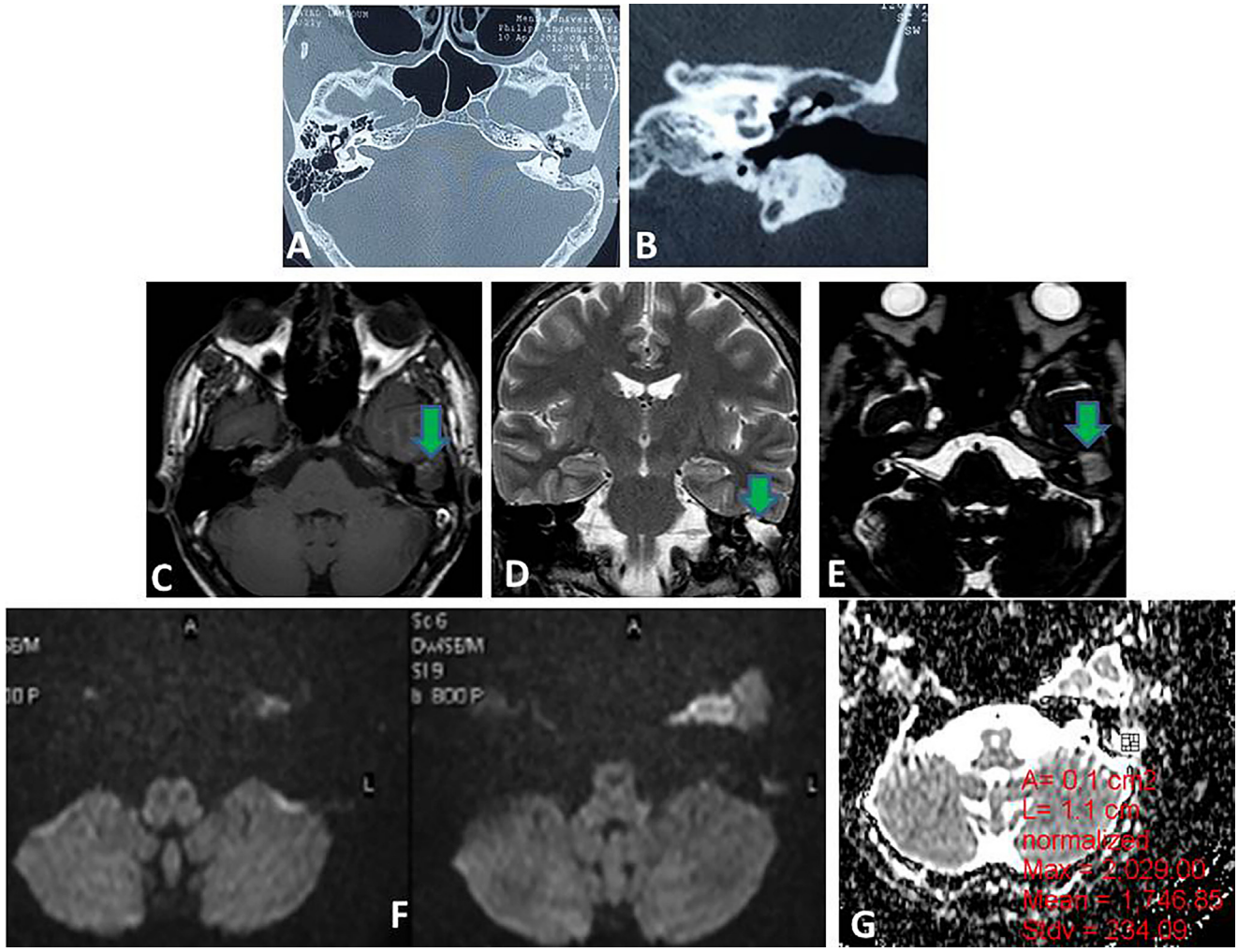

Fig. 7. Left CSOM without cholesteatoma in of a 21 years old man who underwent left CWU middle ear surgery. (A and B) Axial and coronal CT cuts showed complete opacification of the left middle ear cleft by tissue density lesion associated with intact ossicular chain. (C) Axial T1WI, (D) Coronal T2WI, and (E) Axial CISS showed a soft tissue density lesion in the left middle ear cleft of low signal in T1WI and high signal intensity in T2WI and CISS (green arrows). (F) Axial DWI obtained with a b factor of 1000 s/mm^2 showed no high signal intensity at the left middle ear cleft. (G) ADC (mean 1.746.85 $\times$ 10^{-3} mm^2/s).

[14]. Several interpretations to explain the high signal intensity of cholesteatoma on diffusion-weighted images have been proposed. Two mechanisms have been discussed for this high signal intensity: restricted molecular diffusion and T2 shine-through effects. The reason for the increased signal intensity of cholesteatoma on diffusion-weighted MR images is still unknown but seems to be similar to that for the increased signal intensity of epidermoid cysts on diffusion-weighted images [19–21]. Reduced diffusion in cholesteatoma compared with granulation tissue, fibrous tissue, or mucoid secretion is assumed to contribute to high signal intensity of cholesteatoma on diffusion-weighted imaging.

In the present study, diffusion-weighted MR imaging depicted 21ears of surgically proven 20 patients with cholesteatoma. In our series of cases, we did not have any false negative cases but one false positive case in which bone graft used to seal a lateral semicircular canal fistula. This can be explained by the absence of infection in the surgical cavity as all patients with ear drainage received antimicrobials both local and systemic before imaging. This can help eliminate the false positive results that can be met with due to the presence of abscess or infection within the surgical cavity. Artifacts from air-bone and air-tissue interfaces are one of the main drawbacks of DW MRI. Fast SE DW sequences proved better in reducing artifacts observed with echo-planner DW sequences, giving a better spatial resolution and better analysis of the lesions. In recent literature, Aikele et al. [22] reported a sensitivity of 77% (10/13) in detecting residual or recurrent cholesteatoma using the combination of standard MR imaging sequences and DWI missing three small residual cholesteatoma pearls (<5 mm). Specificity, positive and negative predictive values of 100%, 100% and 75% was reported [9]. Another recent report by Stasolla et al. [23] reported a sensitivity of 86% (6/7) detecting recurrent cholesteatoma using echo-planar DWI. In their series only one small cholesteatoma of 2 mm was missed, while the size of the other cholesteatomas varied from 4 to 14 mm. Specificity, positive and negative predictive values of 100%, 100% and 92% were reported [14]. In both studies, included patients were clinically suspected of having residual of recurrent cholesteatoma

Although the results of previous studies [14,16] have proved that comparison of diffusion-weighted images obtained with a b of 800 s/mm^2 without measurement of the apparent diffusion coefficient is sufficient for analysis of the diffusion-weighted sequence [17] we try to assess the benefit of adding ADC values in detecting recurrent cholesteatoma. The current study showed a significant difference in ADCs between postoperative recur-

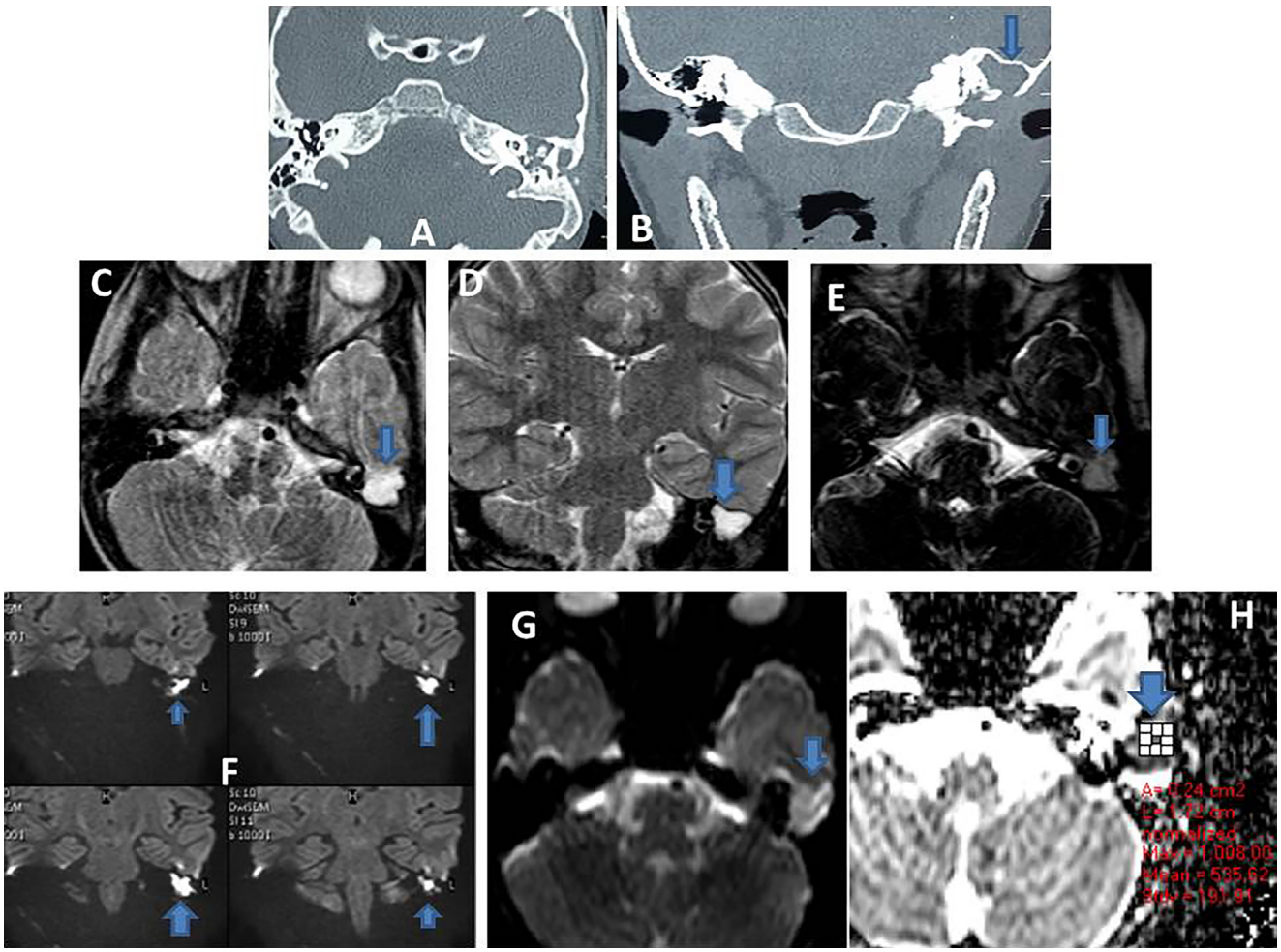

Fig. 8. Recurrent cholesteatoma in the left middle ear of a 12y old woman who underwent CWU middle ear surgery. (A and B) Axial and coronal CT cuts showed complete opacification of the left middle ear cleft by tissue density lesion associated with eroded malleus head and incus body (blue arrow). (C) Axial T2WI, (D) Coronal T2W SE and (E) Axial CISS showed a soft tissue lesion in the left middle ear cleft of high signal intensity at T2WI and CISS. (F) Multiple coronal DWI obtained with a b factor of 1000 s/mm^2 showed high signal intensity of the cholesteatoma (blue arrow). (G) ADC = 595.6385 $\times$ 10^{-3} mm^2/s. The size of the lesion is 15 mm at CT and 10 mm at DWI.

Table 7
ROC curve analysis of ADC values for prediction of recurrent cholesteatoma.

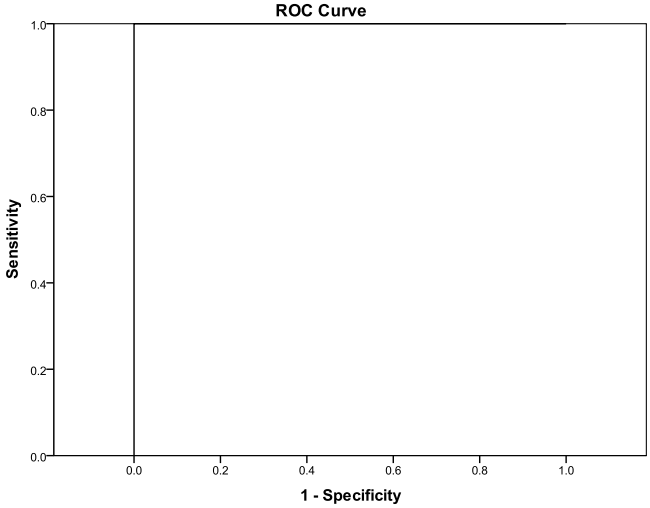

AUC = 1.0 ± 0.001, P = 0.001*.

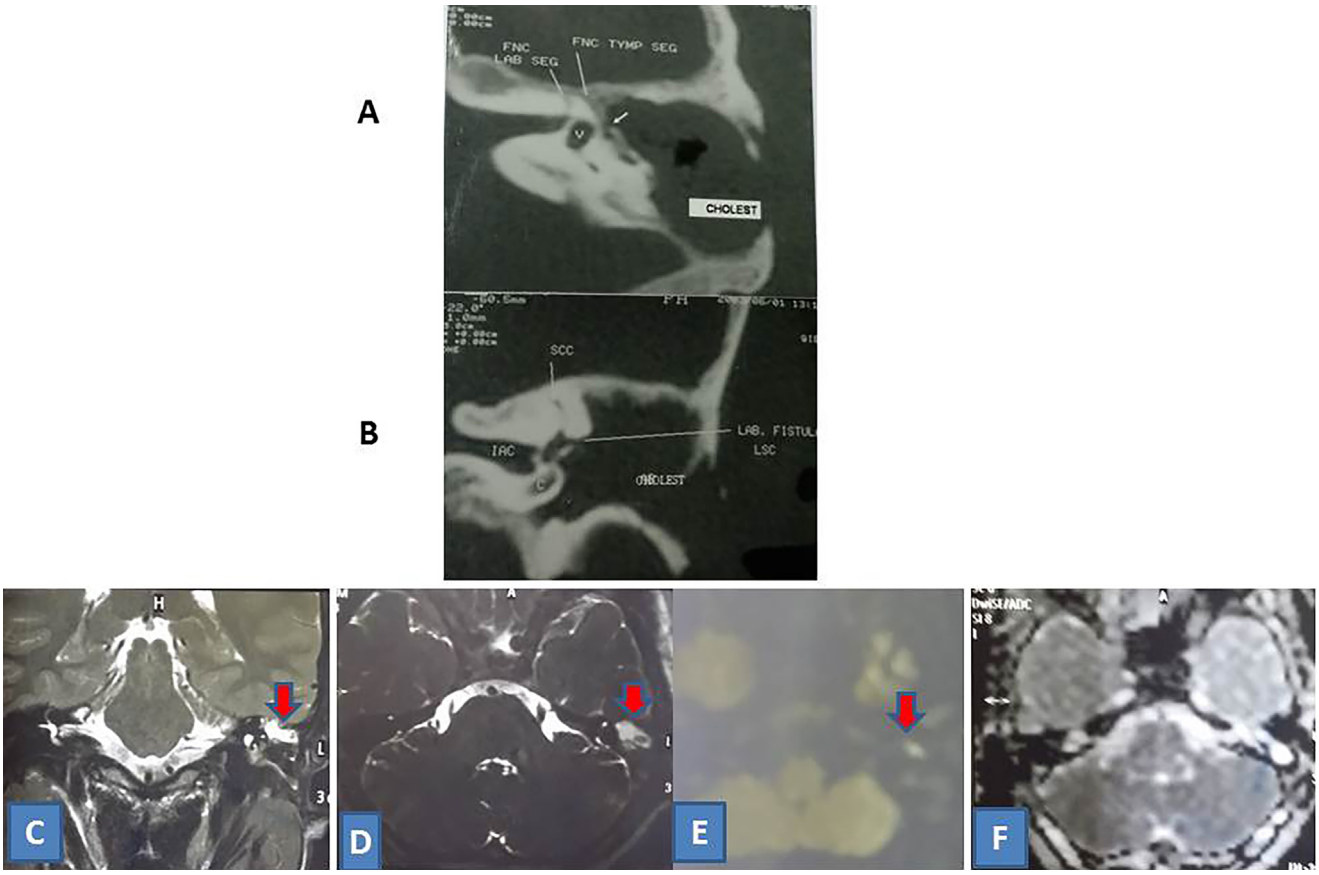

Fig. 9. False positive case of recurrent cholesteatoma in the left middle ear of a 17y old man who underwent left middle ear surgery for a large cholesteatoma complicated by LSC fistula 3years ago. (A and B) Axial and coronal CT cuts showed complete opacification of the right middle ear cleft by large tissue density lesion associated with eroded LSC and tympanic segment of the facial nerve canal (small arrow). (C) Coronal T2WI, (D) Axial CISS showed a soft tissue lesion in the left middle ear cleft of high signal intensity. (E) Axial DWI obtained with a b factor of 1000 s/mm^2 showed small high signal intensity area at the middle ear cleft (red arrow) proved as bone graft sealing LSC fistula. ADC could not measure.

rent cholesteatoma (mean 611.8 ± 51.8) and non-cholesteatoma patients (mean 1638.3 ± 93.5), with the ADC value of cholesteatoma significantly lower than that of non-cholesteatoma. At an optimum ADC cut off value of $\leq 759 \times 10^{-3}$ mm^2/s, it was possible to detect cholesteatoma with good diagnostic performance. This method had good sensitivity and marginally higher specificity with the subjective qualitative method when cholesteatoma demonstrated a signal on the DW images. Maheshwari [24] concluded the ADC of a case report of cholesteatoma patient as 0.58×10^{-3} mm^2/s. Thiriat et al. [25] in his study detect the concordance between the surgical findings and the calculated ADC value of cholesteatoma and suggests that ADC values could be used to allow greater specificity to differentiate cholesteatoma from middle ear abscess or mixed-pattern lesions. Our results are matched with Ravei K et al. [26] who concluded that patient with cholesteatoma were found to have much lower ADCs (median, 707×10^{-6} mm^2/s; interquartile range, $539–858 \times 10^{-6}$ mm^2/s; $P < 0.001$) compared with those that did not have cholesteatoma (median, 1849×10^{-6} mm^2/s; interquartile range, $1574–1982 \times 10^{-6}$ mm^2/s; $P < 0.001$). Our results also concordant with Dr.N.Kailasanathan study [27], who stated that most of cholesteatomas shows ADC values higher than 0.55 however infected cholesteatoma can show low ADC value. DW MRI has 100% sensitivity, 75% specificity, 97.3% PPV and 100% NPV in detecting cholesteatoma [27]

The main limitation of in the sensitivity of the subjective qualitative method is with small recurrent cholesteatoma less than 5 mm, which do not demonstrate a signal high enough to be detected on the DW imaging images. If cholesteatoma is too small to be detected, ADC values cannot be measured or used as a diagnostic tool. However, when an abnormal soft tissue demonstrates a DW imaging signal, our study shows that the use of ADC values can not only detect cholesteatoma with a high sensitivity, but can also improve the confidence levels of the qualitative method when used together.

Table 8
ADC cutoff value of recurrent cholesteatoma.

	Cutoff	Sensitivity	Specificity	PPV	NPP
ADC	≤759	100%	100%	100%	100%

Although specificity was 100% and positive predictive value 95.2% in our study, diffusion-weighted imaging may potentially cause false positive results. High signal intensity in the area of the petrous bone is seen not only with cholesteatomas. Susceptibility artifacts at the air-bone border at the base of the skull, chordomas, cholesterol granulomas, and abscesses may also appear markedly hyperintense on diffusion-weighted imaging. Care should be taken to be aware of the surgical procedures used during the initial surgery before analyzing MR images, especially when a special material such as bone powder has been used.

In conclusion, the advances in MRI techniques are currently changing the preoperative evaluation and the postoperative follow-up protocols for cholesteatoma. DW MRI appears to be an accurate method, as opposed to a standard second-look operation, for the follow-up of patients who have undergone a canal wall up procedure for a chronic otitis media with cholesteatoma.

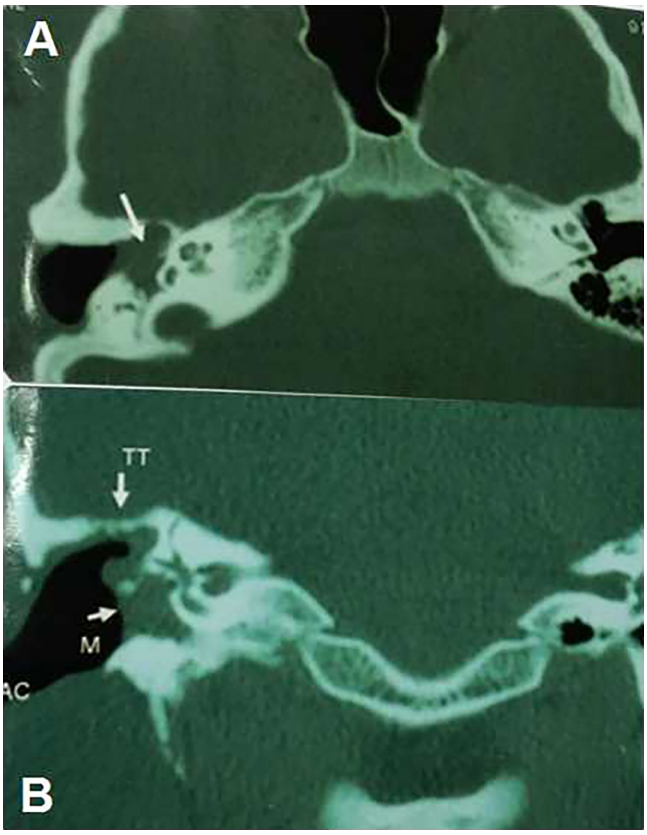

Fig. 10. Recurrent cholesteatoma MDCT of 25 years old man who underwent CWD of the right middle ear surgery. (A) Axial and (B) Coronal CT cuts showed non-dependent tissue density lesion seen extended along the medial wall of the right middle ear cavity with small part of the ossicles engulfed by the lesion which extended through the oval window.

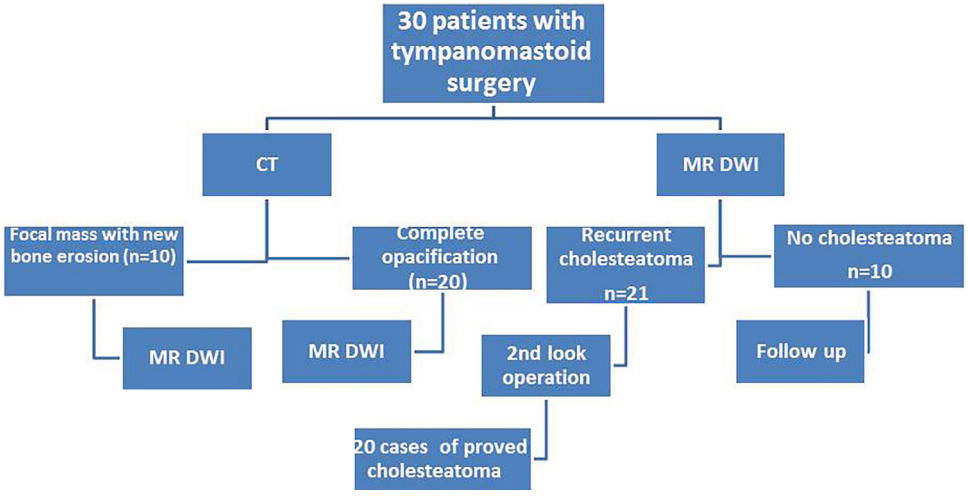

Fig. 11. Flow diagram for description the participants.

5. Conclusion

DW MRI fused with CT is a helpful and effective method for distinguishing cholesteatoma from other soft tissues in post-operative ears. MR DWI sensitivity was 100% and negative predictive value was 100%, which means that patients who show no signs of recurrent cholesteatoma on DW fast SE images may not need second- or third-look surgery. Fusion imaging using HRCT and DW MRI appears to be a promising technique for both the diagnosis and precise localization of cholesteatomas. It provides useful information for surgical planning. The apparent diffusion coefficient (ADC) of postoperative middle ear cholesteatoma is significantly lower than that of noncholesteatomatous tissue.

Conflict of interest

We declare that we have no conflict of interest.

Table 9
Comparison between CT, MRI and operative regarding size of recurrent cholesteatoma.

	CT 10–30 mm	MRI 7–15 mm	Operative size mm
1	25 mm	14 mm	13
2	18 mm	11 mm	11
3	16 mm	10 mm	10
4	10 mm	7 mm	7.3
5	10 mm	8 mm	7.5
6	30 mm	14 mm	14.4
7	15 mm	11 mm	11
8	12 mm	8 mm	8
9	13 m	10 mm	10
10	12 mm	9 mm	9.8
11	18 mm	9.9 m	9.7
12	20 mm	11 mm	11
13	10.5 mm	8 mm	8.2
14	14.5 mm	9.5 mm	9
15	17 mm	10 mm	10
16	10 mm	7 mm	7.4
17	11 mm	8.2 mm	8
18	10 mm	8.8 mm	8.5
19	11.5 mm	9 mm	9
20	12.4 mm	9.5 mm	9.6
21	11.6	8.4 mm	9

Recurrent cholesteatoma	CT	MRI	Operative	P
Range	10–30	7–15	7–14	0.001*
Mean ± SD	14.6 ± 5.2	9.6 ± 2.03	9.5 ± 1.7	

Funding

No disclosure of funding received for this work from any organization.

Author contributions

All authors have apprised the article and actively contributed in the work.

Nasr Mohamed M. Osman: Data collection, technique, image revision, interpretation and final editing.

Ahmed Abdel Rahman: Patients selection, operative data and follow up.

Moustafa Talaat Abdel Hakim Ali: Patients selection, operative data and follow up.

References

[1] P. Aikele, T. Kittner, C. Offergeld, et al., Diffusion-weighted MR imaging of cholesteatoma in pediatric and adult patients who have undergone middle ear surgery, Am. J. Roentgenol. 181 (2003) 261–265.
[2] L. Migirov, S. Tal, A. Eyal, J. Kronenberg, MRI, not CT, to rule out recurrent cholesteatoma and avoid unnecessary second look mastoidectomy, IMAJ 11 (2009) 144–146.
[3] K.M. Schwartz, J.I. Lane, B.D. Bolster Jr., B.A. Neff, The utility of diffusion-weighted imaging for cholesteatoma evaluation, Am. J. Neuroradiol. 32 (3) (2011) 430–436.
[4] M. Lemmerling, B. De Foer, Imaging of cholesteatomatous and non-cholesteatomatous middle ear disease, in: M. Lemmerling, S.S. Kollias (Eds.), Radiology of the Petrous Bone, Springer-Verlag, New York, 2004, pp. 31–47.
[5] S. Kösling, F. Bootz, CT and MR imaging after middle ear surgery, Eur. J. Radiol. 40 (2001) 113–118.
[6] S.P. Blaney, P. Tierney, M. Oyarazabal, D.A. Bowdler, CT scanning in second look combined approach tympanoplasty, Rev. Laryngol. Otol. Rhinol. (Bord.) 121 (2000) 79–81.
[7] B. De Foer, J.P. Vercruysse, B. Pilet, J. Michiels, R. Ver-triest, M. Pouillon, et al., Single-shot, turbo spin-echo, diffusion-weighted imaging versus spin-echo-planar, diffusion-weighted imaging in the detection of acquired middle ear cholesteatoma, Am. J. Neuroradiol. 27 (2006) 1480–1482.
[8] B. De Foer, J.P. Vercruysse, A. Bernaerts, J. Maes, F. Deckers, J.s Michiel, et al., The value of single-shot turbo spin-echo diffusion-weighted MR imaging in the detection of middle ear cholesteatoma, Neuroradiology 49 (2007) 841–848.
[9] F. Más-Estellés, M. Mateos-Fernández, B. Carrascosa-Bisquert, F. Facal de Castro, I. Puchades-Román, C. Morera-Pérez, Contemporary non-echo-planar diffusion-weighted imaging of middle ear cholesteatomas, RadioGraphics 32 (2012) 1197–1213.
[10] Plouin-Gaudon, D. Bossard, C. Fuchsmann, S. Ayari-Khalfallah, P. Froehlich, Diffusion-weighted MR imaging for evaluation of pediatric recurrent cholesteatomas, Int. J. Pediatr. Otorhinolaryngol. 74 (1) (2010) 22–26.
[11] M. Jindal, J. Doshi, M. Srivastav, D. Wilcock, Richard Irving, Ranit De, Diffusion-weighted magnetic resonance imaging in the management of cholesteatoma, Eur. Arch. Otorhinolaryngol. 267 (2010) 181–185.
[12] D. Le Bihan, E. Breton, D. Lallemand, M.L. Aubin, J. Vignaud, M. Laval-Jeantet, Separation of diffusion and perfusion in intravoxel incoherent motion MR imaging, Radiology 168 (2) (1988) 497–505.
[13] F.B. Pizzini, F. Barbieri, A. Beltramello, F. Alessandrini, F. Fiorino, HASTE diffusion-weighted 3-Tesla magnetic resonance imaging in the diagnosis of primary and relapsing cholesteatoma, Otol. Neurotol. 31 (4) (2010) 596–602.
[14] M.F. Dalia, M.R. Sameh, Detection of post-operative residual cholesteatoma using PROPELLER DWI combined with conventional MRI, Egypt. J. Radiol. Nucl. Med. 43 (December) (2012).
[15] F. Keyzer De, D. King Ann, Diffusion-weighted MR imaging in the head and neck diffusion-weighted MR imaging in the head and neck local Harriet C. Thoeny, Radiology 263 (April (1)) (2012).
[16] Adam M. Cassis, Stephin J. Wetmore, Accuracy of CT scan in predicting cholesteatoma in revision of tympanomastoidectomy, Laryngoscope 119 (2009), S1–S184-Supplement S1, page S108.
[17] K.M. Schwartz, J.I. Lane, B.D. Bolster Jr., B.A. Neff, The utility of diffusion-weighted imaging for cholesteatoma evaluation, AJNR Am. J. Neuroradiol. 32 (March (3)) (2011) 430–436, http://dx.doi.org/10.3174/ajnr.A2129, Epub 2010 May 20.
[18] K. Yamashita, T. Yoshiura, A. Hiwatashi, H. Kamano, H. Honda, Ultrashort echo time imaging of normal middle ear ossicles: a feasibility study Crossref Dentomaxillofacial, Radiology 41 (October (1)) (2012).
[19] Riccarda Martina Schuenemann, Gerhard Oechtering Cholesteatoma, After lateral bulla osteotomy in two brachycephalic dogs crossref, J. Am. Anim. Hosp. Assoc. 481 (July) (2012).
[20] R. Souillard-Scemama, F. Dubrulle, Pathologie inflammatoire et infectieuse de la sphère oto-rhinolaryngologique Crossref, EMC – Radiologie et imagerie médicale – Musculosquelettique – Neurologique – Maxillofaciale 7 (June (1)) (2012).
[21] Harriet C. Thoeny, Frederik De Keyzer, Ann D. King, Diffusion-weighted MR imaging in the head and neck diffusion-weighted MR imaging in the head and neck local, Radiology 263 (April (1)) (2012).
[22] P. Aikele, T. Kittner, C. Offergeld, H. Kaftan, K.B. Huttenbrink, M. Laniado, Diffusion-weighted MR imaging of cholesteatoma in pediatric and adult patients who have undergone middle ear surgery, AJR Am. J. Roentgenol. 181 (2003) 261–265.
[23] A. Stasolla, G. Magluilo, D. Parrotto, G. Luppi, M. Marini, Detection of postoperative relapsing/residual cholesteatomas with diffusion-weighted echo-planar magnetic resonance imaging, Otol. Neurotol. 25 (2004) 879–884.
[24] S. Maheshwari, S.K. Mukherji, Diffusion-weighted imaging for differentiating recurrent cholesteatoma from granulation tissue after mastoidectomy: case report, AJNR Am. J. Neuroradiol. 23 (2002) 847–849.
[25] S. Thiriat, S. Riehm, S. Kremer, E. Martin, F. Veillon, Apparent diffusion coefficient values of middle ear cholesteatoma differ from abscess and cholesteatoma admixed infection, AJNR Am. J. Neuroradiol. 30 (June–July) (2009) 1123–1126.
[26] R.K. Lingam, P. Khatri, J. Hughes, A. Singh, Apparent diffusion coefficients for detection of postoperative middle ear cholesteatoma on non-echo-planar, Radiology 269 (2) (2013) 504–510.
[27] N. Kailasanathan, S. Arunprasad, S. Babupeter, The usefulness of diffusion-weighted imaging in cholesteatoma diagnosis and postoperative pathologic correlatioN, Int. J. Latest Res. Sci. Technol. ISSN (Online) 5 (1) (2016) 29–32, ISSN (Online):2278–5299.